Immunology
The Journal of cells, molecules, systems and technologies

British Society for immunology

IMMUNOLOGY ORIGINAL ARTICLE

Tumour-associated changes in intestinal epithelial cells cause local accumulation of KLRG1$^+$ GATA3$^+$ regulatory T cells in mice

Holger Meinicke,[1,2,3] Anna Bremser,[1,2] Maria Brack,[1,2,*] Paulina Akeus,[4] Claire Pearson,[5] Samuel Bullers,[5] Katrin Hoffmeyer,[1] Marc P. Stemmler,[1,†] Marianne Quiding-Järbrink[4] and Ana Izcue[1,2]

[1]*Max Planck Institute of Immunobiology and Epigenetics, Freiburg, Germany,* [2]*Centre for Chronic Immunodeficiency (CCI), University Medical Centre Freiburg and University of Freiburg, Freiburg, Germany,* [3]*Department of Pediatrics and Adolescent Medicine, Division of General Pediatrics, University Medical Centre, Freiburg, Germany,* [4]*Department of Microbiology and Immunology, Institute of Biomedicine, The Sahlgrenska Academy at the University of Gothenburg, Göteborg, Sweden, and* [5]*The Kennedy Institute of Rheumatology, University of Oxford, Headington, Oxford, UK*

doi:10.1111/imm.12750
Received 13 December 2016; revised 13 April 2017; accepted 19 April 2017.
*Present address: Roche AG, Wagistrasse 18, Schlieren 8952, Switzerland.
†Present address: Department of Experimental Medicine I, Nikolaus-Fiebiger Centre for Molecular Medicine, University of Erlangen-Nuremberg, Glueckstrasse 6, Erlangen, Germany.
H.M. and A.B. contributed equally to this work.
Correspondence: Ana Izcue, Max Planck Institute of Immunobiology and Epigenetics, Stübeweg 51, Freiburg D-79108, Germany.
Email: izcue@ie-freiburg.mpg.de
Senior author: Ana Izcue

Summary

CD4$^+$ Foxp3$^+$ regulatory T (Treg) cells include differentiated populations of effector Treg cells characterized by the expression of specific transcription factors. Tumours, including intestinal malignancies, often present with local accumulation of Treg cells that can prevent tumour clearance, but how tumour progression leads to Treg cell accumulation is incompletely understood. Here using genetically modified mouse models we show that ablation of E-cadherin, a process associated with epithelial to mesenchymal transition and tumour progression, promotes the accumulation of intestinal Treg cells by the specific accumulation of the KLRG1$^+$ GATA3$^+$ Treg subset. Epithelial E-cadherin ablation activates the β-catenin pathway, and we find that increasing β-catenin signals in intestinal epithelial cells also boosts Treg cell frequencies through local accumulation of KLRG1$^+$ GATA3$^+$ Treg cells. Both E-cadherin ablation and increased β-catenin signals resulted in epithelial cells with higher levels of interleukin-33, a cytokine that preferentially expands KLRG1$^+$ GATA3$^+$ Treg cells. Tumours often present reduced E-cadherin expression and increased β-catenin signalling and interleukin-33 production. Accordingly, Treg cell accumulation in intestinal tumours from APC$^{min/+}$ mice was exclusively due to the increase in KLRG1$^+$ GATA3$^+$ Treg cells. Our data identify a novel axis through which epithelial cells control local Treg cell subsets, which may be activated during intestinal tumorigenesis.

Keywords: cell surface molecules; mucosa; regulatory T cells; tumour immunology

Introduction

Foxp3-expressing regulatory T (Treg) cells are essential for immune homeostasis, especially in the gut. However, Treg cells can also contribute to pathogenesis, most notably by inhibiting protective immune responses to tumours in mice and humans.[1] Therefore Treg cells must be kept under strict control. Intestinal epithelial cells play

Abbreviations: DSS, dextran sulphate-sodium; HBSS, Hanks' balanced salt solution; IL-33, interleukin-33; Th1, T helper type 1; Treg, CD4$^+$ Foxp3$^+$ regulatory T cells

an active role in immune homeostasis by keeping at bay the intestinal microbiota, and they also participate in the modulation of the immune system.[2–5] However, whether changes in epithelial cells affect gut Treg cells is still unknown.

The Treg cells differentiate into diverse effector subsets that can have organ-specific properties.[6,7] Several effector Treg subsets have been described in the mouse gut, including Helios$^-$ RORγt$^+$ Treg cells, which develop in response to microbial factors, and the GATA3$^+$ Treg subset that arises independently of the microbiota (reviewed in ref. 8). In addition to the expression of distinctive transcription factors, Treg subpopulations can express surface receptors such as KLRG1, which can be found on a significant proportion of gut Treg cells and is considered a marker of terminally differentiated Treg cells.[9,10] In humans, accumulation of effector Treg cells, but not of other FOXP3$^+$ populations, is associated with a worse prognosis in colorectal cancer,[11] and two recent studies have confirmed that human tumour-infiltrating Treg cells have a specific distinct phenotype.[12,13]

Here we use mouse models to examine whether tumour-related alterations of epithelial cells can per se affect intestinal Treg populations. We have focused on E-cadherin, a key epithelial cell adhesion molecule that also affects intracellular signalling. We used a mouse model of cell-specific cadherin switch in which E-cadherin is replaced by its homologue N-cadherin in the intestinal epithelium,[14] mimicking the cadherin switch that takes place during epithelial to mesenchymal transition, a key step in tumour progression. We found that mice with E-cadherin-deficient epithelium present with a striking expansion of effector-like KLRG1$^+$ GATA3$^+$ Foxp3$^+$ cells. Using additional genetically modified mouse models, we linked KLRG1$^+$ GATA3$^+$ Treg cell accumulation to increased epithelial β-catenin signals, which promote intestinal interleukin-33 (IL-33) expression. Spontaneous intestinal tumours from mice with increased β-catenin signals also presented strong specific accumulation of KLRG1$^+$ GATA3$^+$ Treg cells. Our data highlight an unappreciated role for intestinal epithelial cells in controlling the size of the gut Treg cell compartment. Given the role of Treg cells in maintaining an immunosuppressive environment in tumours, the axis linking epithelial β-catenin to KLRG1$^+$ GATA3$^+$ Treg cell accumulation could be an interesting therapeutic target.

Materials and methods

Mouse strains

Wild-type C57BL/6, C57BL/6 Cdh1$^{Ncad/fl}$ Villin Cre$^+$,[14] congenic B6.SJL-*Cd45*, BALB/c *Il10*$^{-/-}$, C57BL/6 *Rag2*$^{-/-}$ and Ctnnb1$^{(Ex3)fl/+}$ Lgr5-EGFP-IRES-ERT2:Cre$^+$[15,16] mice were kept and bred under specific pathogen-free or germ-free conditions at the animal facility of the Max-Planck Institute of Immunobiology and Epigenetics. For tamoxifen treatment, Ctnnb1$^{(Ex3)fl/+}$ Lgr5-EGFP-IRES-ERT2:Cre$^+$ mice and controls were injected intraperitoneally every other day with 200 μg/day tamoxifen in sunflower oil for a total of three doses, and analysed 22 days after the last injection. All experiments were approved by the institutional review board of the Max Planck Institute of Immunobiology and Epigenetics and the local government in Freiburg. APC$^{min/+}$ mice on a C57BL/6 background were kept and bred under specific pathogen-free conditions in filter-top cages at the University of Gothenburg and analysed between 18 and 21 weeks of age. The study was approved by the animal ethics committee at the University of Gothenburg.

Isolation of leucocytes from the lamina propria and epithelial cells

Leucocytes from the lamina propria were isolated as described elsewhere.[17,18] Briefly, small intestine and colon were removed and cleaned. Samples (around 5 mm long) were removed for histology, and the rest of the colon was used for lymphocyte isolation. For young Cdh1$^{\Delta IEC}$ mice and littermate controls, the whole small intestine was used for lymphocyte isolation after removal of samples for histology. For IL-10-deficient and dextran sulphate-sodium (DSS) -treated mice and controls, the distal small intestine was used for lymphocyte isolation. The proximal and distal parts of Ctnnb1$^{(Ex3)fl/+}$ Lgr5-EGFP-IRES-ERT2:Cre$^+$ mice and controls were used for isolation as indicated. For APC$^{min/+}$ and control mice, the entire small intestine was used for isolation. After washing with ice-cold PBS, intestines were washed twice in Hanks' balanced salt solution (HBSS) containing 5 mM EDTA and 10 mM HEPES at 37° to remove the epithelial cell layer. The tissue was then minced finely and digested three times in HBSS containing Dispase (5 units/ml; BD Biosciences, Franklin Lakes, NJ, USA), Collagenase IV (0·5 mg/ml; Worthington, Lakewood, NJ) and DNaseA (0·5 mg/ml; AppliChem, Darmstadt, Germany), at 37° with constant shaking. Supernatants were collected and lymphocytes were enriched after a gradient centrifugation using buffered Percoll (GE Healthcare, Freiburg, Germany).

DSS-colitis

Induction of colitis using DSS was done as previously described.[19] Briefly, animals were given 3% DSS (MP Biomedicals, Santa Ana, CA) in the drinking water for 8 days. Weight loss was monitored as a sign of disease progression. Mice were killed at day 8 for analysis and the establishment of colitis was checked by macroscopic signs (swollen, pale colon).

Antibodies and flow cytometry

Single-cell suspensions were stained in 96-well plates (10^6 cells per well). The following conjugated antibodies were purchased from eBioscience (Affymetrix, Inc., Santa Clara, CA, USA): TCR-β (H57-597), CD3 (145-2C11), CD4 (GK 1..5), KLRG1 (2F1), CD103 (2E7), CD44 (IM7), CD45RB (C363.16A), CD62L (MEL-14), CD69 (H1.2F3), CD45.1 (A20), CD45.2 (104), CD25 (PC61.5), Foxp3 (FJK-16s), GATA3 (TWAJ), Tbet (3C8), Rorγ (B2D), Helios (22F6), IRF4 (3E4), Ki67 (20Raj1), Nur77 (12.14) and CTLA4 (UC10-4B9). Anti-IL-33Rα antibody (DIH9) was purchased from Biolegend (San Diego, CA, USA). Intracellular staining was performed with the eBioscience permeabilization and fixation kit. Anti-Bcl-2 (3F11) was purchased from BD Biosciences. Dead cells were excluded by staining with Fixable Viability Dye (eBioscience). For cytokine staining, cells were incubated for 4 hr at 37° in the presence of PMA, ionophore and Brefeldin A as described elsewhere,[18] and stained with antibodies against IL-2 (JES6-5H4), IL-5 (TRFK5), IL-13 (13A), IL-17 (17B7) or interferon-γ (2E2). All flow cytometry experiments were acquired using a BD LSR II cytometer or LSR Fortessa (BD). FlowJo Version 8.8.7 was used for data analysis. For calculating total cell numbers, cell concentrations were counted with a CASY cell counter (Roche, Basel, Switzerland) and the total numbers multiplied by the frequency of $CD4^+$ $Foxp3^+$ cells among living cells.

Treg cell culture

Flat-bottom 96-well plates were pre-coated with 5 μg/purified anti- mouse CD3ε (145-2C11, Biolegend) at 37° for a minimum of 30 min. FACS-sorted $CD4^+$ $CD25^+$ cells from wild-type C57BL/6 were seeded at 10^5 cells/well and cultured in RPMI-1640 containing 10% fetal calf serum and 1 U/ml IL-2 or 5 ng/ml/IL-33 where indicated (PeproTech, Hamburg, Germany). After 8 hr or 3 days of incubation at 37°, cells were harvested and analysed by flow cytometry. To test *in vitro* suppression, 10^5 $CD4^+$ $CD25^-$ T cells were cultured with 10^5, 5×10^4 or 10^4 $CD4^+$ $CD25^+$ $KLRG1^-$ or $CD4^+$ $CD25^+$ $KLRG1^-$ cells in the absence of exogenous IL-2.

Quantitative real-time PCR

Intestinal epithelial cells were isolated after 37° incubation with RPMI/5%FCS/2·5 mM EDTA. Total RNA was extracted with TRI reagent (Sigma-Aldrich, St Louis, MO, USA) and was reverse-transcribed with QuantiTect Reverse Transcription Kit (Qiagen, Hilden, Germany) following the instructions of the manufacturer. Amplification was performed using Absolute Blue qPCR SYBR low ROX mix (Thermo Fisher Scientific, Waltham, MA, USA). Values were normalized to *Hprt*. Primer sequences were taken from refs. 20 (*Il33*) and 21 (*Hprt*).

Statistical analysis

Statistical analysis was performed using GraphPad Prism using a two-tailed unpaired Student's *t*-test when only two groups were tested, or analysis of variance with Bonferroni-Post-test where more than two groups were tested. Differences were considered statistically significant when $P < 0{\cdot}05$. Bars represent arithmetic mean except for bars in graphs with a logarithmic *y*-axis, which represent the median.

For the analysis of genes altered in the intestinal cadherin switch model, GSE81920 was analysed using the Multiplot module from GenePattern.[22] Genes with cytokine activity were identified with AmiGO Gene Ontology term GO:0005125, *Mus musculus*.[23]

Results

Ablation of E-cadherin on intestinal epithelial cells induces $KLRG1^+$ Treg cell accumulation in the gut

We used a model of gut-specific cadherin replacement that mimics the cadherin switch observed during epithelial to mesenchymal transition in oncogenic progression.[14] In our model, one E-cadherin allele is replaced by N-cadherin whereas the other allele is floxed and conditionally deleted in intestinal epithelial cells after expression of an intestinal epithelial cell-restricted Villin-Cre transgene ($Cdh1^{fl/NcadKI}$ $VilCre^+$, denoted $Cdh1^{\Delta IEC}$ mice). In the absence of Cre expression, N-cadherin is co-expressed together with E-cadherin in all E-cadherin-expressing organs; this ectopic N-cadherin expression does not detectably affect the mouse phenotype.[14] In $VilCre^+$ mice where E-cadherin is deleted in intestinal epithelial cells, N-cadherin preserves cell adhesion and the intercellular junctions in the gut epithelium,[14] although the mice develop intestinal inflammation (manuscript in preparation). Nevertheless, we observed that the frequencies of T helper type 1 (Th1) (IFN-γ^+), Th2 (IL-5^+) and Th17 (IL-$17A^+$) effector $CD4^+$ T cells were not increased in the gut from $Cdh1^{\Delta IEC}$ mice compared with control littermates (Fig. 1a). The frequency of IL-2^+ $CD4^+$ T cells was also not increased in the gut from $Cdh1^{\Delta IEC}$ mice; actually, the frequency of IL-2-expressing $CD4^+$ T cells was reduced compared with controls in the gut, but not in lymphoid organs (Fig. 1a, and see Supplementary material, Fig. S1). In contrast, when we examined the $Foxp3^+$ T-cell (Treg) compartment in $Cdh1^{\Delta IEC}$ mice, we found a striking increase in the frequency of Treg cells in the small intestine and colon, with a smaller accumulation in spleen and mesenteric lymph nodes (Fig. 1b). Neither the co-expression of E-cadherin and N-cadherin ($Cdh1^{fl/Ncad}$ mice) nor

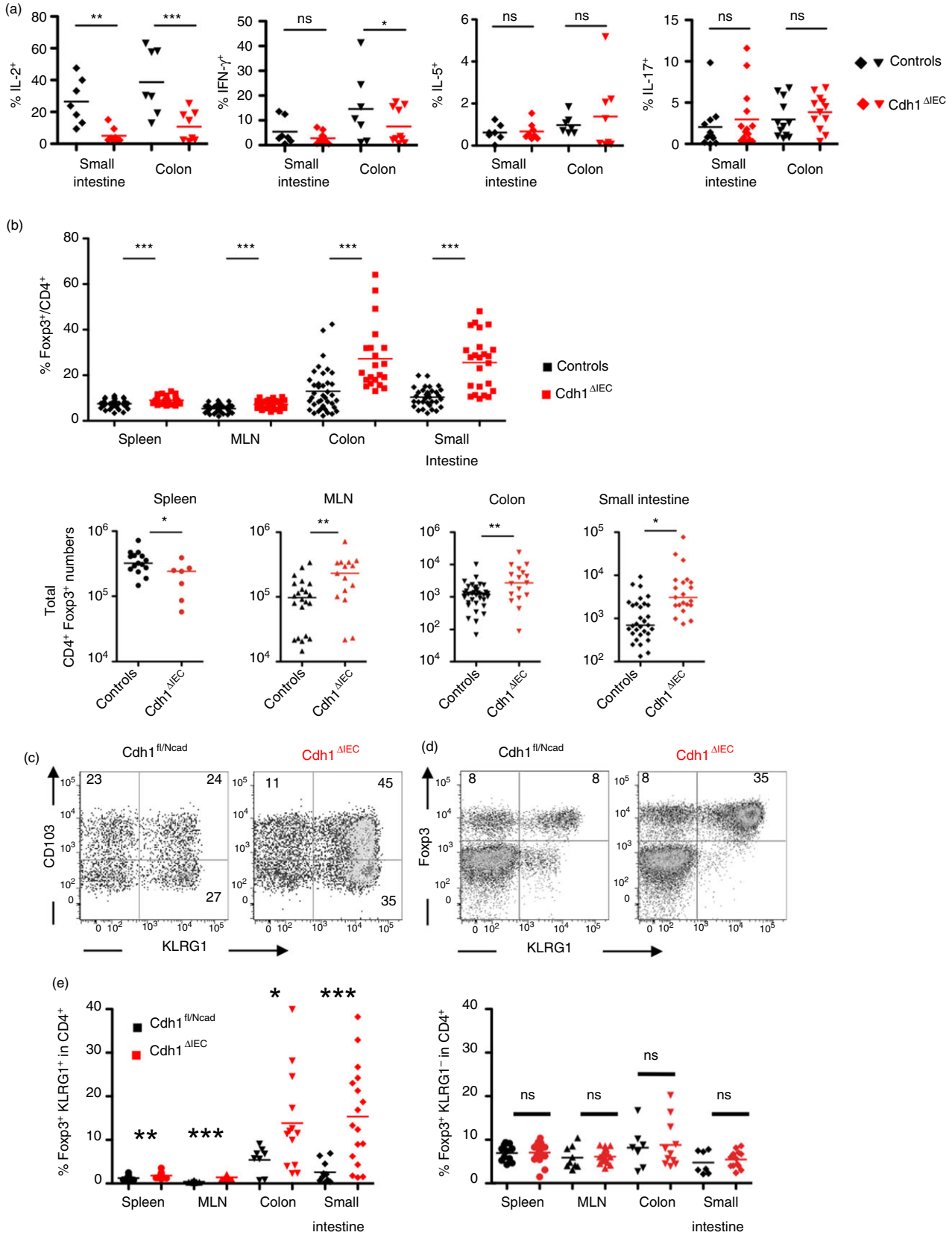
(a)
% IL-2+
% IFN-γ+
% IL-5+
% IL-17+
Small intestine
Colon
ns
Controls
Cdh1 ΔIEC
(b)
% Foxp3+/CD4+
Spleen
MLN
Colon
Small Intestine
Total CD4+ Foxp3+ numbers
(c)
Cdh1 fl/Ncad
Cdh1 ΔIEC
CD103
KLRG1
(d)
Foxp3
(e)
% Foxp3+ KLRG1+ in CD4+
% Foxp3+ KLRG1− in CD4+

Figure 1. Regulatory T (Treg) cells expressing the E-cadherin receptor KLRG1 accumulate in the gut of $Cdh1^{\Delta IEC}$ mice (a) Cytokine production by $CD4^+$ $Foxp3^-$ T cells from the small intestine or colon of $Cdh1^{\Delta IEC}$ mice or control littermates. Data are pooled from two (interleukin-2; IL-2) or three (interferon-γ; IFN-γ, IL-5, IL-17A) independent experiments. (b) Top row, $Foxp3^+$ frequencies among $CD4^+$ T cells in $Cdh1^{\Delta IEC}$ mice or control littermates. Bottom row, absolute numbers of $Foxp3^+$ $CD4^+$ cells in $Cdh1^{\Delta IEC}$ mice and control littermates. (c) Representative plots of KLRG1 versus CD103 expression among $CD4^+$ $Foxp3^+$ T cells from the colonic lamina propria of $Cdh1^{\Delta IEC}$ mice and control littermates. (d) Representative plots of KLRG1 versus Foxp3 expression among $CD4^+$ T cells from colonic lamina propria of $Cdh1^{\Delta IEC}$ mice and control littermates. (e) Frequencies of $Foxp3^+$ $KLRG1^+$ (left) or $Foxp3^+$ $KLRG1^-$ (right) among $CD4^+$ T cells in the indicated organs in $Cdh1^{\Delta IEC}$ mice or control littermates. Black symbols, $Cdh1^{fl/Ncad}$ controls; red symbols, $Cdh1^{\Delta IEC}$ mice. All mice were analysed at the age of 3 weeks, because the lethality observed in $Cdh1^{\Delta IEC}$ mice precluded analysis at later time-points. Mice of both sexes were used for the analyses. Each point corresponds to an individual mouse. $*P < 0{\cdot}05$; $**P < 0{\cdot}01$; $***P < 0{\cdot}001$; ns, not significant compared with $Cdh1^{fl/Ncad}$ controls.

mono-allelic E-cadherin deletion ($Cdh1^{fl/+}$ $VilCre^+$ mice) affected the frequency of $Foxp3^+$ cells (see Supplementary material, Fig. S1a). $Cdh1^{\Delta IEC}$ mice are runty and about half the size of their littermates.[14] Their smaller spleen size, which corresponds with their smaller body size (manuscript in preparation), probably explains the lower cell numbers and total Treg cell numbers observed in the spleen from $Cdh1^{\Delta IEC}$ mice (Fig. 1b). In contrast, despite their smaller body size, absolute Treg cell numbers were increased in the mesenteric lymph nodes and gut from $Cdh1^{\Delta IEC}$ mice compared with littermates (Fig. 1b).

We then determined the expression of the CD103 and KLRG1 on the accumulating Treg cells. Both CD103 and KLRG1 have been proposed as markers of activated Treg cells; in addition, both receptors can recognize E-cadherin. $KLRG1^+$ cells, irrespective of CD103 co-expression, were drastically increased among colonic $Foxp3^+$ cells in $Cdh1^{\Delta IEC}$ mice (Fig. 1c, and see Supplementary material, Fig. S1b), although there was a trend towards reduction of $CD103^+$ $KLRG1^-$ cells and the frequency of total CD103 cells was unchanged. In fact, the increase in Treg cell frequency among $CD4^+$ T cells was mainly the result of increased $KLRG1^+$ Treg cell frequency in all organs, and the frequency of $KLRG1^-$ Treg cells was, in contrast, unaffected (Fig. 1d,e). This suggests that epithelial E-cadherin typically restrains the accumulation of $KLRG1^+$ Treg cells in the gut, and that epithelial loss of E-cadherin leads to local accumulation of $KLRG1^+$ Treg cells.

Although Treg cell accumulation was strongest in the gut, the frequency of $KLRG1^+$ $Foxp3^+$ Treg cells was elevated in all organs observed, pointing to a general increase in Treg cells rather than altered migration of Treg cells to the intestine. Interestingly, the elevated $KLRG1^+$ frequency was specific for $Foxp3^+$ T cells, as the frequency of $KLRG1^+$ cells in other T-cell populations was not changed (see Supplementary material, Fig. S1c). $KLRG1^+$ Treg cells have been shown to accumulate in some models of inflammation.[24,25] However, there was no specific accumulation of $KLRG1^+$ Treg cells in two classical models of colitis that we tested, microbiota-independent acute DSS-induced inflammation and the microbiota-dependent, chronic colitis that develops in IL-10-deficient mice (Fig. 2). This indicates that intestinal inflammation does not necessarily result in increased levels of $KLRG1^+$ Treg cells.

Accumulating $KLRG1^+$ $Foxp3^+$ T cells have a $GATA3^+$ effector Treg cell phenotype

In humans, three populations of FOXP3-expressing cells have been described: naive Treg, effector Treg, and $FOXP3^+$ cells without regulatory activity (non-Treg).[26] These populations are associated with differential clinical outcomes in cancer. High levels of $FOXP3^+$ effector Treg cells in colorectal cancer tumours are associated with a poor prognosis, whereas high levels of $FOXP3^+$ non-Treg cells are associated with a better prognosis,[11] underscoring the contribution of functional Treg cells to development/maintenance of tumours. Populations of effector Treg cells and populations of $Foxp3^+$ cells producing inflammatory cytokines have also been described in mice.[27,28]

We therefore sought to characterize the accumulating $KLRG1^+$ Treg cells in $Cdh1^{\Delta IEC}$ mice. $KLRG1^+$ $Foxp3^+$ T cells have been described as terminally differentiated effector Treg cells with suppressive activity *in vivo* and *in vitro*[9,24,25] (see Supplementary material, Fig.S2a). To determine whether the $KLRG1^+$ Treg population in $Cdh1^{\Delta IEC}$ mice is phenotypically equivalent to the described populations of $KLRG1^+$ Treg cells, or whether it results from KLRG1 induction on different Treg subpopulations, we performed a phenotypic analysis of $KLRG1^+$ Treg cells isolated from the mesenteric lymph nodes of $Cdh1^{\Delta IEC}$ and control littermates. As previously described,[24] $KLRG1^+$ Treg cells exhibited a phenotype consistent with activated/effector Treg cells, characterized by expression of CTLA-4, IRF4 and Helios, low levels of Bcl-2, high levels of CD44 and low levels of CD62L (Fig. 3a,b, and see Supplementary material, Fig. S2b–e). $KLRG1^+$ Treg cells were enriched for proliferative $Ki67^+$ cells at a similar extent in $Cdh1^{\Delta IEC}$ and control mice, suggesting that E-cadherin does not affect $KLRG1^+$ Treg cell proliferation in this model (Fig. 3c). Although $KLRG1^+$ and $KLRG1^-$ Treg

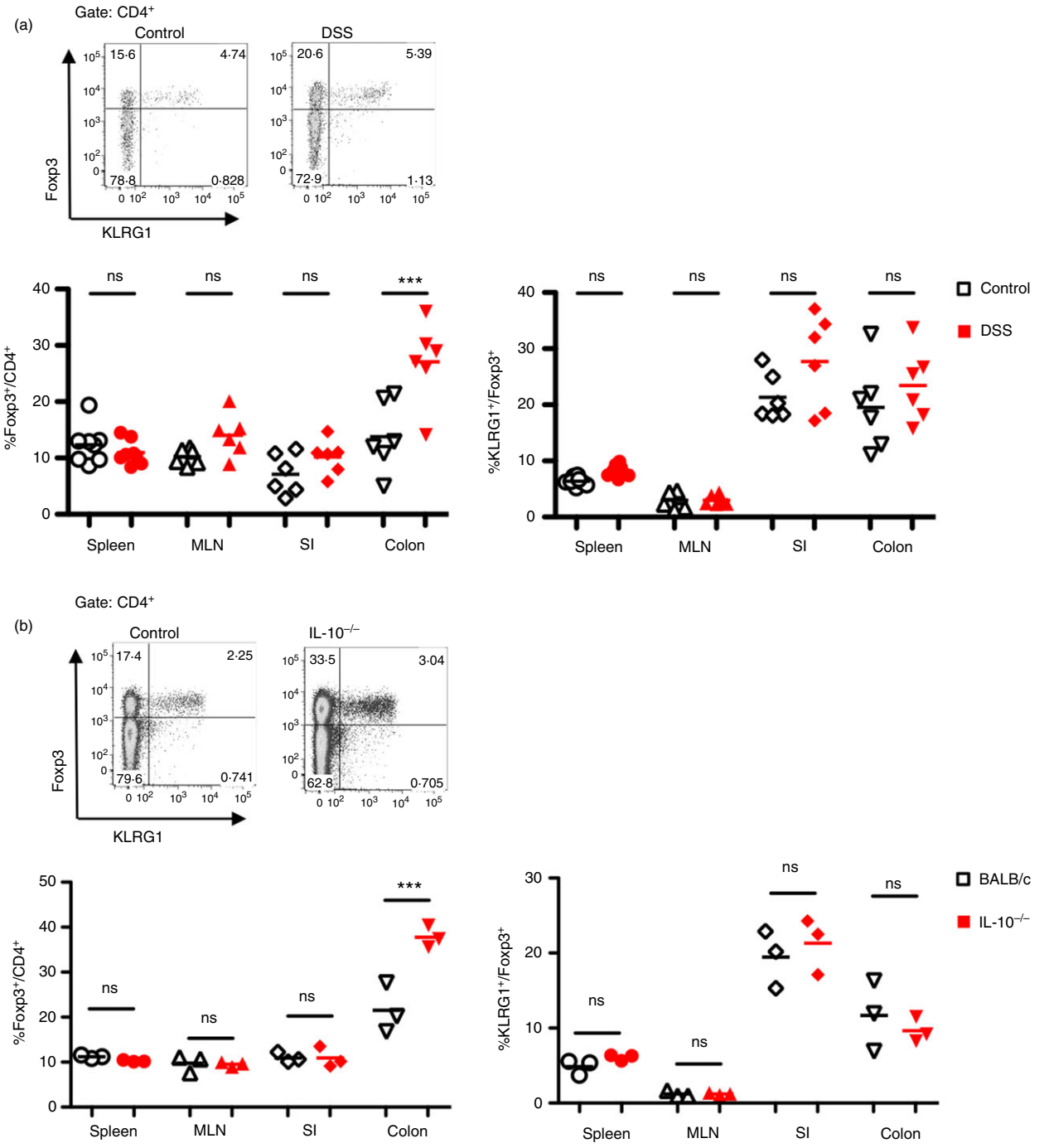

Figure 2. Inflammation does not drive specific KLRG1$^+$ regulatory T (Treg) cell accumulation. (a) Treg populations in DSS-treated mice. Eight- to nine-week-old mice were treated for 8 days with 3%DSS or water, and analysed immediately after the treatment stopped. Top: the plot shows representative KLRG1 and Foxp3 expression among TCRβ^+ CD4$^+$ T cells from the colonic lamina propria and untreated control mice. Bottom left, frequencies of Foxp3$^+$ cells among CD4$^+$ in the indicated organs. Bottom right, frequencies of KLRG1$^+$ cells among CD4$^+$ Foxp3$^+$ cells in the indicated organs. Data are pooled from two independent experiments with three mice per group/experiment. Both females and males were used. (b) Treg cell populations in interleukin-10 (IL-10) -deficient mice and control littermates. Data show one representative experiment out of two; plots as in (a). Each point corresponds to an individual mouse; 8-week-old IL-10-deficient mice (two females, one male) and sex-matched heterozygous littermates were used. ***$P < 0{\cdot}001$; ns, not significant compared to controls.

populations clearly phenotypically differed from each other, cadherin switch did not affect the phenotype of the KLRG1$^+$ Treg subpopulation, suggesting that the absence of E-cadherin does not induce KLRG1 across all Treg cell subsets, but instead increases the accumulation of the KLRG1$^+$ effector Treg cell subset.

Effector Treg cells have been further divided into subpopulations expressing transcription factors mirroring the other CD4$^+$ T helper subsets, such as T-bet, GATA3 and RORγt.[6,8] The expression of the transcription factor GATA3 in intestinal Treg cells was mostly restricted to KLRG1$^+$ cells in Cdh1$^{\Delta IEC}$ and control mice (Fig. 3d,e), whereas we did not find a correlation of the transcription factors T-bet and RORγt with KLRG1 expression in Treg cells (Fig. 3d,e), suggesting that GATA3 expression is mainly limited to KLRG1$^+$ Treg cells.

GATA3 expression is essential for the anti-inflammatory activity of the GATA3$^+$ subset of Treg cells,[29–31] but high levels of GATA3 can turn a Treg cell into a *bona fide* Th2 pro-inflammatory T cell.[32] Interestingly, the expression of GATA3 by Treg cells in Cdh1$^{\Delta IEC}$ mice was lower than in the small GATA3$^+$ fraction among Foxp3$^-$ T cells (Fig. 3e), fitting with Treg-like rather than Th2-like GATA3 expression. Similar to genuine Treg cells, KLRG1$^+$ Treg cells expressed high levels of Foxp3 (Fig. 3e), and did not produce any of the pro-inflammatory cytokines we tested (Fig. 3f, and see Supplementary material, Fig. S2f). Hence, they do not correspond to the human pro-inflammatory FOXP3$^+$ fraction but to a *bona fide* effector subset.

In summary, the KLRG1$^+$ Treg population accumulating in the gut of Cdh1$^{\Delta IEC}$ mice is phenotypically similar to the one in control Cdh1$^{fl/Ncad}$ and wild-type mice. KLRG1$^+$ Foxp3$^+$ cells display an activated GATA3$^+$ Treg cell phenotype with high levels of Foxp3 like *bona fide* Treg cells, suggesting that epithelial-specific cadherin switching induces the local accumulation of a subset of effector Treg cells rather than naive Treg or inflammatory Treg cells.

Increased β-catenin signals induce the accumulation of KLRG1$^+$ Treg cells in the gut

Cdh1$^{\Delta IEC}$ mice show alterations in the epithelial β-catenin pathway, with β-catenin target genes already increased in epithelial cells from newborn Cdh1$^{\Delta IEC}$ mice.[14] We set out to determine if alterations in β-catenin also increase the frequency of intestinal Treg cells. β-catenin binds to cadherins at the cell membrane, but detached β-catenin can translocate into the nucleus and activate Wnt target genes (reviewed in ref. 33). The activation of the Wnt/β-catenin pathway is a hallmark of intestinal tumours. To determine if the increased levels of β-catenin signals observed in epithelial cells after cadherin switch can induce the accumulation of intestinal Treg cells, we used a model of tamoxifen-induced recombination in intestinal stem cells that deletes the β-catenin exon required for tagging the protein for degradation.[15,16] Upon recombination, a stable form of β-catenin is generated that can signal in the absence of Wnt ligands, and the progeny of the recombined intestinal stem cells therefore exhibits constitutive β-catenin signalling.

We analysed the mice 3 weeks after the tamoxifen injection, when active β-catenin accumulates in the nucleus. We found that enhanced β-catenin signals increased Treg cell accumulation in the small intestine of adult mice (Fig. 4a), and also increased the accumulation of KLRG1$^+$ Treg cells (Fig. 4b). Indeed, the increased Treg cell frequency was due to an augmentation in KLRG1$^+$ Foxp3$^+$ T cells, whereas no differences were seen in the proportions of KRLG1$^-$ Foxp3$^+$ cells (Fig. 4c,d), similar to the pattern observed in mice with epithelium-specific cadherin switch. In keeping with the published regional variations of β-catenin activation,[16] KLRG1$^+$ Treg cell accumulation was more marked in the small intestine compared with the colon. As in Cdh1$^{\Delta IEC}$ mice, the KLRG1$^+$ Treg cells were GATA3$^+$ (Fig. 4e). Hence, increased β-catenin signalling in intestinal epithelial cells recapitulates the KLRG1$^+$ Foxp3$^+$ Treg cell accumulation observed in Cdh1$^{\Delta IEC}$ mice.

Intestinal tumours from APC$^{min/+}$ mice accumulate KLRG1$^+$ Treg cells

β-Catenin signals are often increased in tumour cells of epithelial origin, including intestinal tumours.[34] On the other hand, Treg cells accumulate in many types of tumours, where they can suppress the cytotoxic antitumoral response.[6,35] To assess whether KLRG1$^+$ Treg cells are also specifically increased in a model of spontaneous gut tumour development with enhanced β-catenin signalling, we analysed the Treg populations in intestinal tumours from APC$^{min/+}$ mice.[36] These mice have a heterozygous mutation in *Apc*, a gene encoding an essential protein to target β-catenin for proteosomal degradation that is mutated in around 80–90% of human colorectal cancer tumours.[37] Upon spontaneous mutations in the second *Apc* allele, β-catenin is stabilized and aging APC$^{min/+}$ mice therefore spontaneously develop intestinal tumours, primarily in the small intestine (reviewed in ref. 38). It has been previously shown that Treg cells accumulate in these tumours and impair cytotoxic responses.[39] In accordance with published data, we found that most tumours had increased Treg cell frequencies (Fig. 5a). When we analysed KLRG1 expression in these mice, we found that KLRG1$^+$ GATA3$^+$ Treg cells were predominant among Treg cells from the tumours, but not from the surrounding tissue (Fig. 5b,c). As in mice with cadherin switch or with an epithelial-specific increase in β-catenin, the increased Treg cell frequency in intestinal tumours from APC$^{min/+}$ mice was exclusively due to an increase in the KLRG1$^+$ Treg cell population (Fig. 5d,e). In accordance with the other models with increased β-catenin signals, the frequency of KLRG1$^+$ Foxp3$^+$ Treg cells was increased but the percentage of KLRG1$^-$ Foxp3$^+$ Treg cells remained unchanged. The mice without Treg cell accumulation in tumours ('Treg^{lo} tumors') did not show increased KLRG1$^+$ Treg cells either. Hence, enhanced β-catenin

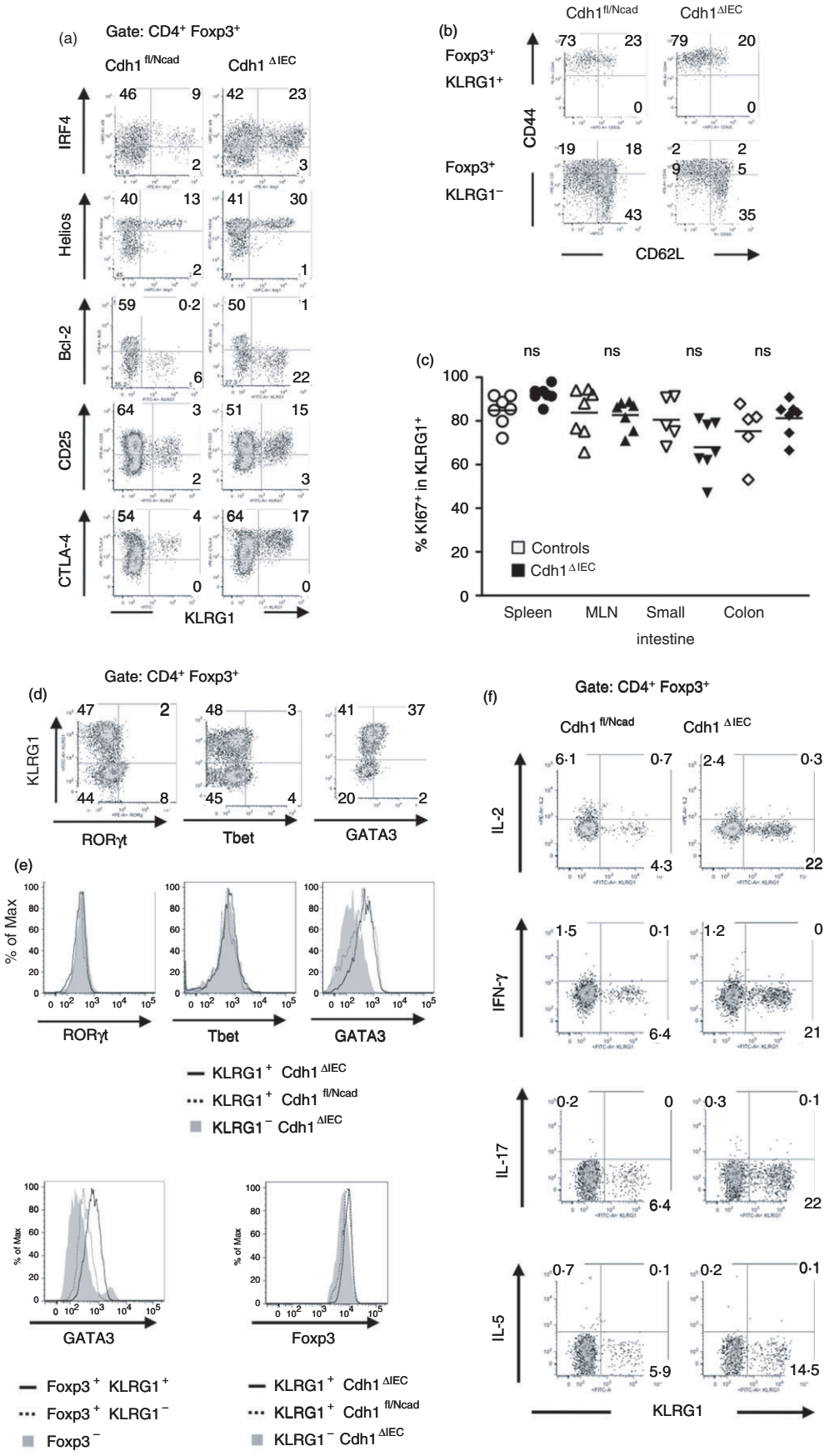
(a)
Gate: CD4+ Foxp3+
Cdh1 fl/Ncad
Cdh1 ΔIEC
IRF4
Helios
Bcl-2
CD25
CTLA-4
KLRG1
(b)
Cdh1fl/Ncad
Cdh1ΔIEC
Foxp3+ KLRG1+
Foxp3+ KLRG1−
CD44
CD62L
(c)
ns
% KI67+ in KLRG1+
Controls
Cdh1ΔIEC
Spleen
MLN
Small intestine
Colon
(d)
Gate: CD4+ Foxp3+
KLRG1
RORγt
Tbet
GATA3
(e)
% of Max
RORγt
Tbet
GATA3
KLRG1+ Cdh1ΔIEC
KLRG1+ Cdh1fl/Ncad
KLRG1− Cdh1ΔIEC
GATA3
Foxp3
Foxp3+ KLRG1+
Foxp3+ KLRG1−
Foxp3−
KLRG1+ Cdh1ΔIEC
KLRG1+ Cdh1fl/Ncad
KLRG1− Cdh1ΔIEC
(f)
Gate: CD4+ Foxp3+
Cdh1 fl/Ncad
Cdh1 ΔIEC
IL-2
IFN-γ
IL-17
IL-5
KLRG1

Figure 3. KLRG1$^+$ regulatory T (Treg) cells have an E-cadherin-independent activated phenotype and belong to the GATA3$^+$ Treg cell subset. (a) KLRG1 versus the indicated activation markers in CD4$^+$ Foxp3$^+$ lymphocytes from the mesenteric lymph nodes (MLN) of control Cdh1$^{fl/Ncad\ KI}$ (left) and littermate Cdh1$^{\Delta IEC}$ mice. (b) CD44 and CD62L expression among Foxp3$^+$ KLRG1$^+$ (top) and Foxp3$^+$ KLRG1$^-$ (bottom) CD4$^+$ T cells from the MLN of control Cdh1$^{fl/NcadKI}$ (left) and littermate Cdh1$^{\Delta IEC}$mice. (c) Frequency of proliferating Ki67$^+$ cells among MLN KLRG1$^+$ CD4$^+$ Foxp3$^+$ T cells. Each symbol shows data from a single mouse, data are pooled from three independent experiments. (d) Expression of RORγt, Tbet and GATA3 in CD4$^+$ Foxp3$^+$ cells isolated from the colonic lamina propria of Cdh1$^{\Delta IEC}$ mice. Plots are representative of three independent analyses. (e) Expression of lineage-defining transcription factors in Foxp3$^+$ KLRG1$^+$ CD4$^+$ T cells from the colonic lamina propria. Top: cells from Cdh1$^{\Delta IEC}$ (continuous line) and littermate Cdh1$^{fl/Ncad}$ (dotted line) compared with CD4$^+$ Foxp3$^+$ KLRG1$^-$ T cells from the same Cdh1$^{\Delta IEC}$ mouse (grey solid histogram). Bottom left: GATA3 expression in KLRG1$^+$ (dotted line) and KLRG1$^-$ (continuous line) Foxp3$^+$ CD4$^+$ T cells compared with Foxp3$^-$ CD4$^+$ T cells (grey solid histogram). Bottom right: Foxp3 e-pression in T cell subsets as in top. (f) interleukin-2 (IL-2), interferon-γ (IFN-γ), IL-5 and IL-17A secretion by CD4$^+$ Foxp3$^+$ cells from the MLN of control Cdh1$^{fl/NcadKI}$ (left) and littermate Cdh1$^{\Delta IEC}$ (right) mice. All data shown are representative of two or three independent experiments with at least one 3-week-old Cdh1$^{\Delta IEC}$ and one littermate control Cdh1$^{fl/NcadKI}$ mice. Mice of both sexes were used for the analyses.

signalling also drives the specific accumulation of the KLRG1$^+$ GATA3$^+$ Treg cell subset in spontaneous intestinal tumours.

Interleukin-33 is induced in epithelial cells with increased β-catenin activity and promotes KLRG1$^+$ accumulation

To identify a molecule that could mediate the communication between β-catenin signals in epithelial cells and accumulation of KLRG1$^+$ Treg cells, we compared the mRNA expression profile of intestinal epithelial cells from young Cdh1$^{\Delta IEC}$ and control mice, focusing on genes with cytokine or chemokine activity. The analysis identified the alarmin *Il33* as a gene specifically increased in epithelial cells lacking E-cadherin (Fig. 6a). Interleukin-33 is known to be up-regulated in APC^{min} tumours,[20] and we found that increased β-catenin signals also promote IL-33 induction in the intestinal epithelium (Fig. 6b,c). Hence, IL-33 is induced in epithelial cells with activated β-catenin.

Interleukin-33 promotes the accumulation of GATA3$^+$ Treg cells in the intestine,[40] and KLRG1$^+$ Treg cells express high levels of the IL-33 receptor upon stimulation (Fig. 6d). Accordingly, IL-33 induced the accumulation of KLRG1$^+$ Treg cells *in vitro* (Fig. 6e). The accumulation was due to the expansion of existing KLRG1$^+$ Treg cells, as IL-33 did not induce KLRG1 expression on KLRG1$^-$ Treg cells upon culture (Fig. 6f). Interleukin-33 favoured KLRG1$^+$ Treg cell division as well as accumulation of undivided cells (Fig. 6g), indicating that it can enhance both proliferation and survival of KLRG1$^+$ Treg cells. Hence, our data indicate that IL-33 can link malignancy-associated epithelial changes to the accumulation of a specific Treg cell subset in mouse intestine.

Discussion

Treg cells in the gut are controlled by local factors,[8] but the role of epithelial cells in this cross-talk, and how tumoral changes affect intestinal Treg cells, is less well understood. Our results indicate that changes associated with tumour progression, namely cadherin switching and increased β-catenin activity, cause effector Treg cell accumulation in the gut.

Beyond their functions in cell–cell adhesion, cadherins also affect intracellular signals. E-cadherin directly binds the Wnt pathway mediator β-catenin, and a previous report showed that β-catenin transcriptional targets are increased in our model of intestinal cadherin switch.[14] Using a model of induced epithelial β-catenin signalling,[16,41] we found that increased β-catenin signals in epithelial cells recapitulate the KLRG1$^+$ Treg cell accumulation found in the cadherin switch model. Hence, the altered epithelial signals resulting from reduced E-cadherin can promote the specific accumulation of KLRG1-expressing Treg cells. We have identified IL-33 as a likely candidate to mediate GATA3$^+$ KLRG1$^+$ Treg cell accumulation in response to increased epithelial β-catenin signals. The frequency of IL-2-expressing CD4$^+$ T cells was not increased, but rather decreased, in Cdh1$^{\Delta IEC}$ mice. Although IL-2 plays an important role in Treg cell maintenance, it is not the only factor that drives Treg cell accumulation. The fact that IL-2 is not increased in the gut of Cdh1$^{\Delta IEC}$ mice suggests that other factors drive Treg cell maintenance in this setting. We find that IL-33 is increased in epithelial cells with ablated E-cadherin expression or increased β-catenin signals, as well as in epithelial cells from APC^{min} tumours,[20] and that it directly promotes KLRG1$^+$ Treg cell survival and proliferation. It will be of interest to assess the levels of IL-33 in different models of intestinal inflammation, such as Th2-driven models or in the DSS model, and to check its effect on KLRG1$^+$ Treg cell accumulation in these settings. Whether β-catenin directly induces IL-33, or whether the increase in IL-33 is secondary to changes induced by β-catenin signalling, remains to be investigated.

Cadherin switch, β-catenin signals, and Treg cell accumulation are all linked to cancer. Treg cells often accumulate in human and mouse tumours, and they are considered to contribute to the immunosuppressive environment that protects tumours from immune attack.[1]

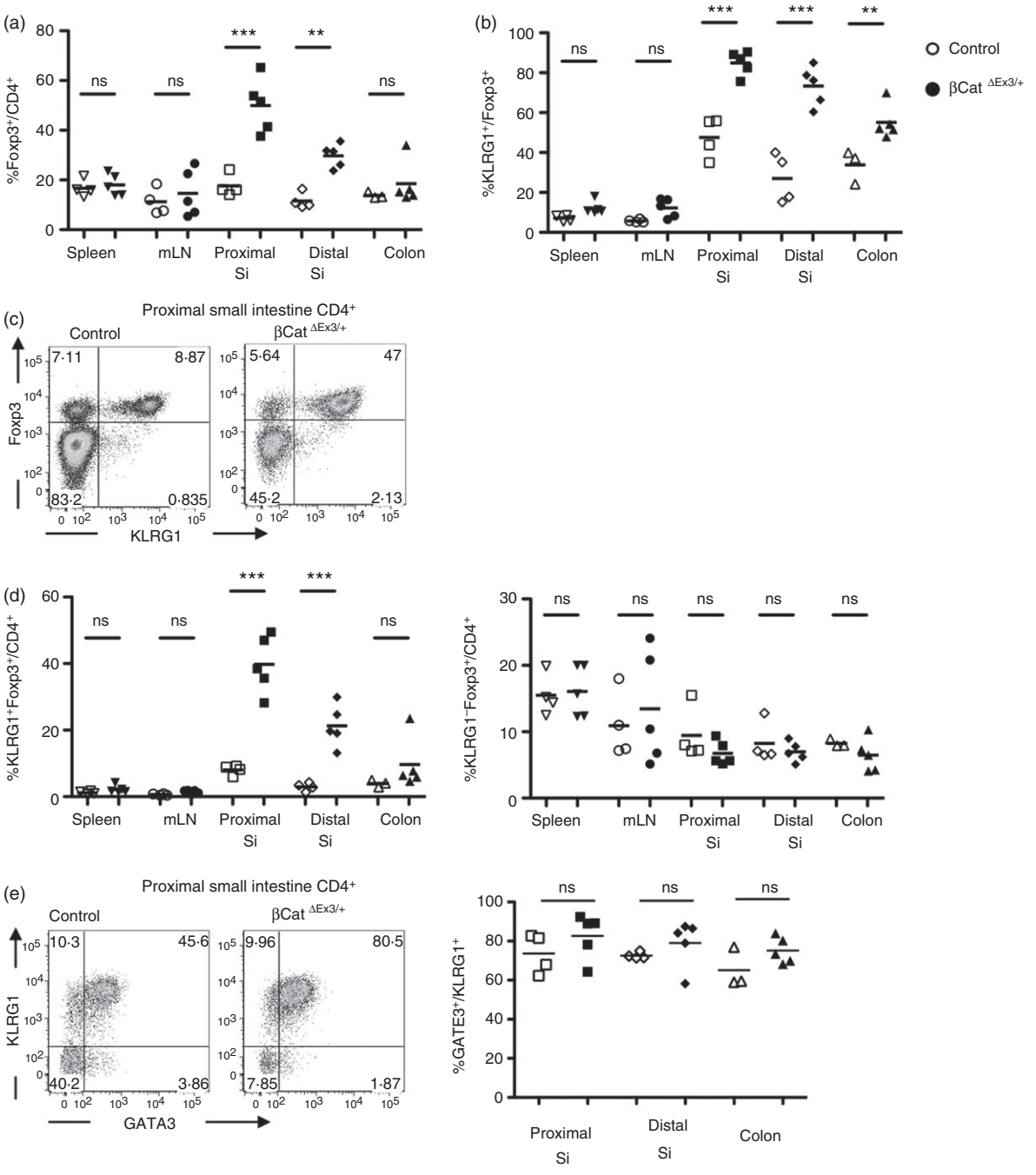

Figure 4. Epithelial β-catenin expands the intestinal regulatory T (Treg) cell compartment through the accumulation of KLRG1$^+$ Treg cells. (a) Frequency of Foxp3$^+$ among CD4$^+$ T cells from tamoxifen-treated mice with the active β-catenin construct (filled; Ctnnb1$^{(Ex3)fl/+}$ Lgr5-EGFP-IRES-ERT2:Cre$^+$, called here βCat$^{\Delta Ex3/+}$) and control mice (empty; Ctnnb1$^{+/+}$ Lgr5-EGFP-IRES-ERT2:Cre$^+$ or Ctnnb1$^{(Ex3)fl/+}$). (b) Frequency of KLRG1$^+$ cells among Foxp3$^+$ CD4$^+$ T cells from mice as in (a). (c) Representative plots of KLRG1 and Foxp3 expression in CD4$^+$ T cells from the proximal small intestinal lamina propria. (d) Frequency of Foxp3$^+$ KLRG1$^+$ (left) or Foxp3$^+$ KLRG1$^-$ (right) among CD4$^+$ T cells from mice as in (a). (e) Representative plot of GATA3 expression in proximal small intestinal lamina propria Foxp3$^+$ CD4$^+$ T cells from mice as in (a), and frequencies of GATA3$^+$ cells among intestinal KLRG1$^+$ Foxp3$^+$ cells. Data shown are from two independent experiments. Eight- to nine-month-old mice of both sexes were used. Each point represents an individual mouse, with a total of four control and five βCat$^{\Delta Ex3/+}$ mice. ***$P < 0{\cdot}001$; **$P < 0{\cdot}01$; ns, not significant.

Indeed, in human colorectal cancer effector Treg cell accumulation is associated with a worse disease-free outcome.[11] Here we show that Treg cell accumulation in spontaneous tumours in the APC$^{min/+}$ model, which is known to inhibit the accumulation of effector T cells,[39] is exclusively due to KLRG1$^+$ GATA3$^+$ Treg cells. We do

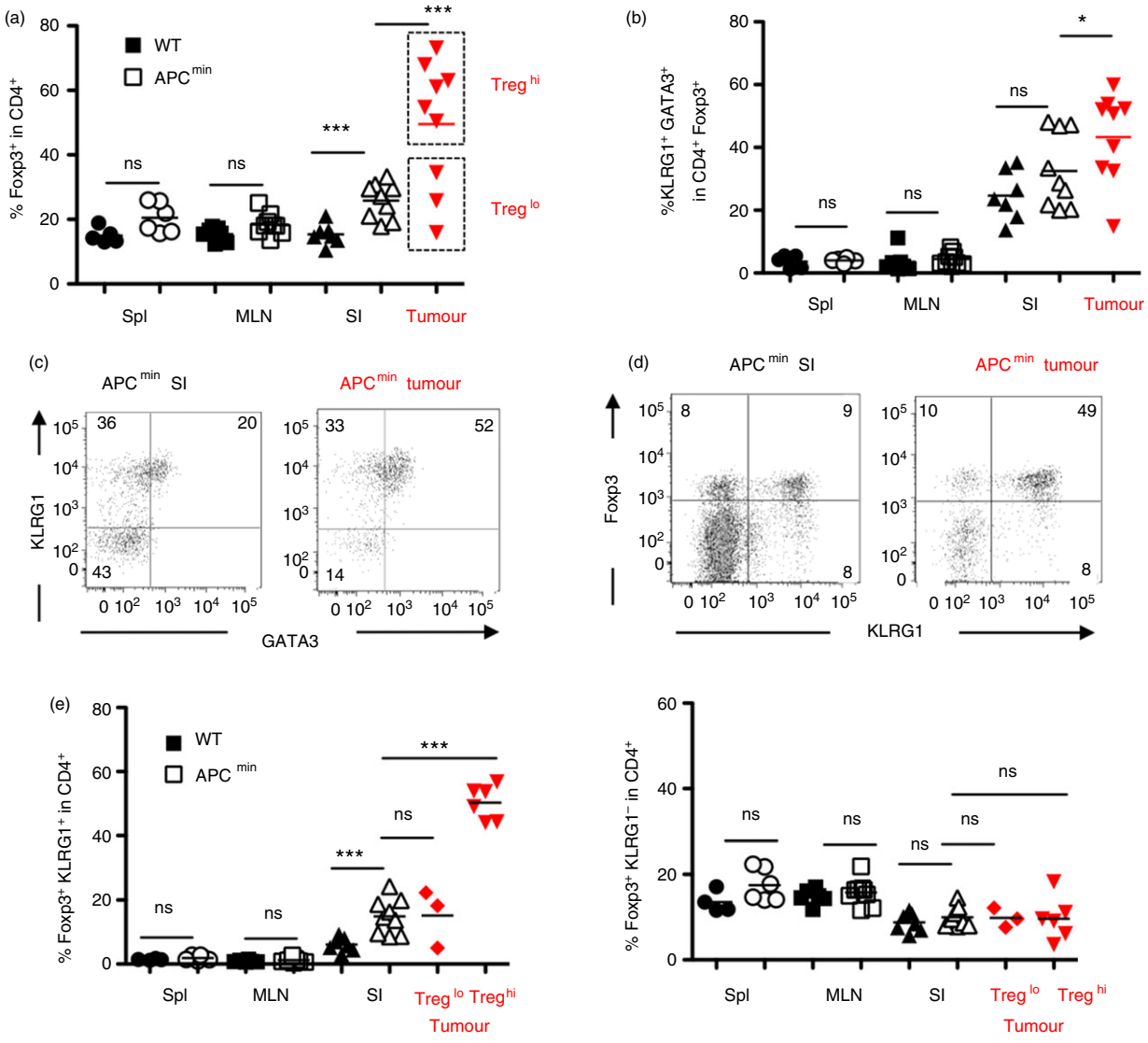

Figure 5. Intestinal tumours promote the accumulation of KLRG1$^+$ regulatory T (Treg) cells. (a) Frequency of Foxp3$^+$ cells among CD4$^+$ T cells from APC$^{min/+}$ (filled black symbols), intestinal tumours of APC$^{min/+}$ (filled red symbols) and control mice (empty symbols). Dashed boxes indicate tumours with (Treg^{hi}) or without (Treg^{lo}) accumulation of Foxp3$^+$ T cells. (b) Frequencies of KLRG1$^+$ GATA3$^+$ cells among CD4$^+$ Foxp3$^+$ and (c) representative plot of KLRG1 and GATA3 expression in Foxp3$^+$ CD4$^+$ T cells from the indicated organs of mice as in (a). (d) Representative plots of KLRG1 and Foxp3 expression in CD4$^+$ T cells from the indicated organ and (e) frequency of Foxp3$^+$ KLRG1$^+$ (left) or Foxp3$^+$ KLRG1$^-$ (right) among CD4$^+$ T cells from mice as in (a). Data shown are from three independent experiments. Each point represents an individual mouse, a total of seven control and nine APC$^{min/+}$ mice were used. Mice were 18–21 weeks old when analysed. Mice from both sexes were used for this study. Small intestinal tumours with a diameter between 1 and 4 mm were analysed ***$P < 0{\cdot}001$; *$P < 0{\cdot}05$; ns, not significant.

not know the exact process leading to the local accumulation of KLRG1$^+$ GATA3$^+$ Treg cells. KLRG1$^+$ Treg cell frequencies in Cdh1$^{\Delta IEC}$ mice were increased in all organs analysed, suggesting that migration is not the mechanism leading to Treg cell accumulation. Accordingly, IL-33 increased KLRG1$^+$ Treg cell numbers and frequencies in an *in vitro* model, where migration is excluded. We found that IL-33 increases both proliferation and survival of existing KLRG1$^+$ cells *in vitro*. Since KLRG1$^+$ Treg cells in newborn mouse intestine have already a high proliferation rate, as shown in Fig. 3(c), it is plausible that in the Cdh1$^{\Delta IEC}$ model the major effect of IL-33 is enhancing KLRG1$^+$ Treg cell survival.

The specific accumulation of a particular effector Treg cell subset in tumours could have consequences beyond immunosuppression. GATA3$^+$ Treg cells have been proposed to induce tissue repair through the secretion of amphiregulin.[42,43] Amphiregulin binds the epidermal

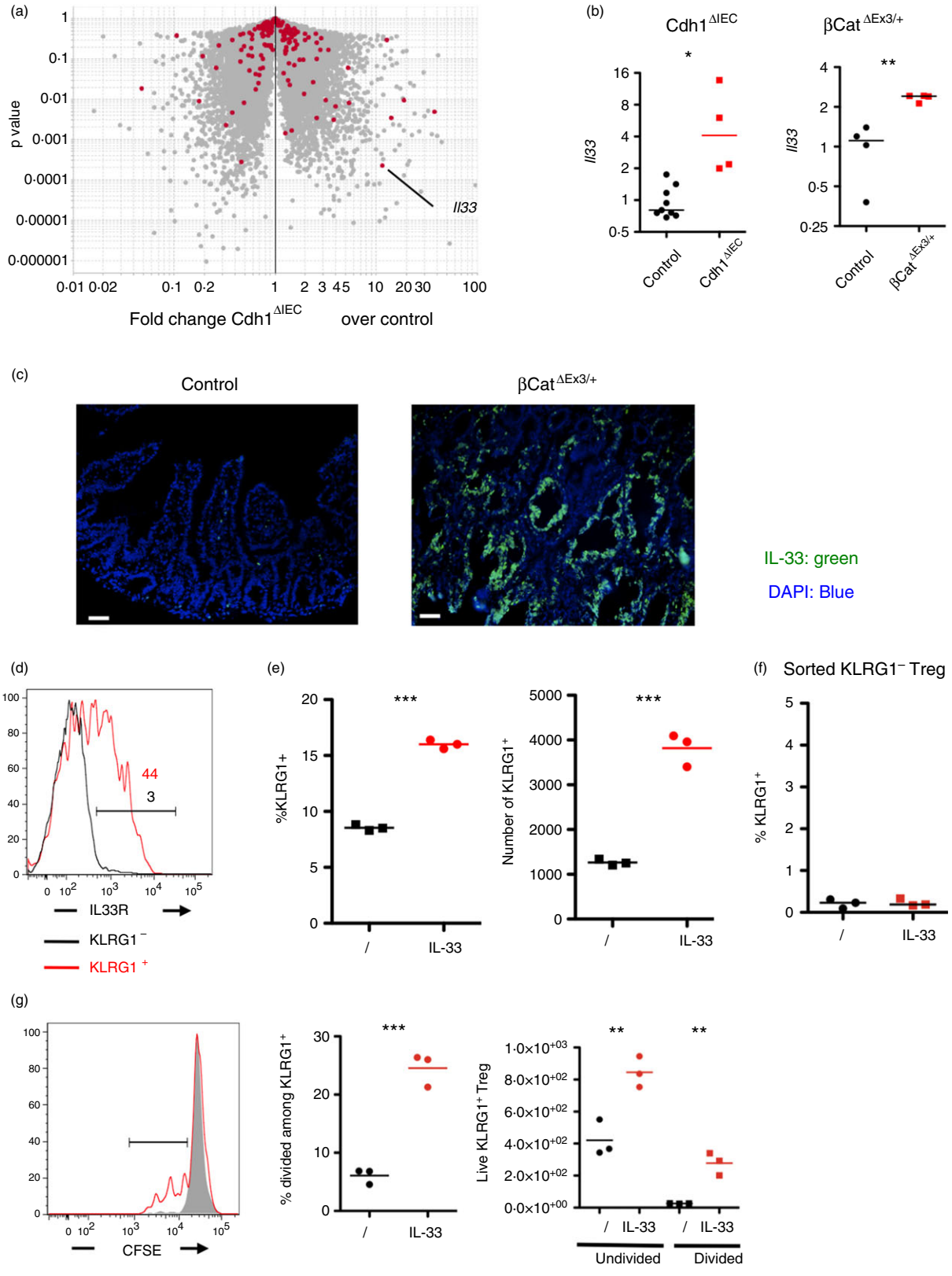

growth factor receptor, which promotes growth of numerous cancers,[44] so it is possible that Treg cells accumulating in tumours promote carcinogenesis not only through immunosuppression but also by secreting factors supporting cancer cell survival. Along this line, KLRG1$^+$ Treg cells are enriched for β_8 integrin and have an enhanced capacity

Figure 6. Increased β-catenin signals induce interleukin-33 (IL-33) in intestinal epithelial cells. (a) Volcano plot showing fold change versus statistical significance of genes expressed in intestinal epithelial cells from 2-week-old $Cdh1^{\Delta IEC}$ mice compared with control littermates, as analysed by microarray (GSE81920). Each dot represents one transcript. Genes highlighted in red are those with cytokine activity (Gene Ontology term GO:0005125, *Mus musculus*) (b) *Il33* expression in intestinal epithelial cells from $Cdh1^{\Delta IEC}$ mice (3-week-old) and control littermates or $\beta Cat^{\Delta Ex3/+}$ and control mice, as measured by quantitative PCR. $\beta Cat^{\Delta Ex3/+}$ and control samples were taken from mice analysed in Fig. 4. Each dot represents one mouse. Values are normalized to *Hprt* expression in each sample. (c) Interleukin-33 expression in small intestine from control (left) or $\beta Cat^{\Delta Ex3/+}$ (right) mice. Tissue was taken from the mice analysed in Fig. 4. Bar represents 50 μm. (d) Expression of IL-33 receptor on activated $KLRG1^+$ (red line and number) and $KLRG1^-$ (black line and number) regulatory T (Treg) cells. Sorted C57BL/6 $CD25^+$ T cells were stimulated for 3 days with plate-bound anti-CD3 and stained for Foxp3, KLRG1 and IL-33 receptor. Histograms are gated on Viability Dye^- $CD4^+$ $Foxp3^+$ $KLRG1^+$ or $KLRG1^-$ cells. Numbers show the frequency of IL-33 receptor-positive cells. Data are representative of two independent experiments. (e) Frequency (left) and total numbers (right) of $KLRG1^+$ cells among $CD4^+$ $Foxp3^+$ live cells 3 days after culture of sorted C57BL/6 Treg cells with anti-CD3 with or without 5 ng/ml of IL-33. (f) Frequency of $KLRG1^+$ cells after sorted C57BL/6 $KLRG1^-$ Treg were cultured as in (e). Cultures are representative of 2–4 independent experiments each. $^{***}P < 0{\cdot}001$; $^{**}P < 0{\cdot}01$; $^{*}P < 0{\cdot}05$. (g) Sorted $KLRG1^+$ Treg cells were labelled with CFSE and mixed 1 : 10 with $KLRG1^-$ Treg. Cells were cultured as in (e). Left, representative plot of CFSE signal in cells cultured with (red line) or without (grey histogram) IL-33. Bar shows divided cells. Centre, frequency of divided cells among live $KLRG1^+$. Right, total numbers of divided and undivided live cells. Data are representative of two independent experiments.

to activate transforming growth factor-β,[45] which also favours the oncogenic process. It will be of interest to check whether Treg cells equivalent to mouse $KLRG1^+$ $GATA3^+$ Treg cells accumulate in human tumours. Because IL-33 is an alarmin expressed by different tissues,[46] the processes described here may play a role in tuning immune regulation in tumours from various organs.

Our results show that increased β-catenin signals promote accumulation of $KLRG1^+$ Treg cells, resulting in a strong increase in $Foxp3^+$ frequencies. Our present findings complement reports on the regulation of tissue repair by $KLRG1^+$ Treg cells,[42,43] stressing the bidirectional interaction between the immune system and epithelia, and highlight an unappreciated role for intestinal epithelial cells in controlling the size of the gut Treg cell compartment. This may be important to ensure that protective immunity against invading pathogens is retained. Tumour-associated epithelial changes disrupt this process, which results in the local accumulation of a specific effector Treg cell subset, underscoring how epithelial cells are important for the maintenance of a balance among $CD4^+$ T-cell populations in the gut. Furthermore, our findings provide mechanistic insight into how the accumulation of immunosuppressive effector Treg populations is mediated following epithelial changes. Given the enormous clinical utility of strategies that target pathways inhibiting intratumoral immune responses, our data identify a novel target that could potentially be manipulated to inhibit Treg cell accumulation in tumours with fewer of the deleterious side effects associated with current frontline therapeutics.

Acknowledgements

H.M., A.B. and M.B. performed the experiments involving $Cdh1^{\Delta IEC}$ and $KLRG1^{-/-}$ mice, A.B. and A.I. performed the *in vitro* cultures, P.A. and M.Q-J. performed the $APC^{min/+}$ experiments, C.P. and S.B. performed the IL-33 staining on gut sections, and A.B. and K.H. performed stable β-catenin mouse strain experiments. M.S. analysed data and contributed essential reagents, A.I. directed research and wrote the paper with A.B. and input from all the authors. We thank members of the Izcue laboratory for helpful discussions and comments on the manuscript, P. Rauf for help during the initial work, K. Maloy for critical reading of the manuscript and R. Kemler for advice and material. Villin-Cre mice were generously provided by S. Robine. We are indebt to R. Hussong for outstanding technical help. We thank C. Johner, A. Ogboro, M. Pfunder, U. Stauffer, S. Burkart and the rest of the mouse facility staff for excellent animal care, and A. Wuerch, S. Hobitz and K. Schuldes for cell sorting. This work was supported by the Bundesministerium für Bildung und Forschung (BMBF 01 EO 0803) and by the Max Planck Society. M. Q-J. and P.A. are supported by the Swedish Research Council and the Swedish Cancer Foundation. C.P. and S.B. are supported by the Kennedy Trust. H.M. was supported by a Walter Hitzig fellowship of the Centre of Chronic Immunodeficiency, University Hospital Freiburg. A.B. is a member of the IMPRS-MCB, a joint international PhD programme of the Max Planck Institute of Immunobiology and Epigenetics and the University of Freiburg, Germany.

Disclosures

The authors report no conflicting interest.

References

1 Nishikawa H, Sakaguchi S. Regulatory T cells in cancer immunotherapy. *Curr Opin Immunol* 2014; **27**:1–7.
2 Gallo RL, Hooper LV. Epithelial antimicrobial defence of the skin and intestine. *Nat Rev Immunol* 2012; **12**:503–16.
3 Peterson LW, Artis D. Intestinal epithelial cells: regulators of barrier function and immune homeostasis. *Nat Rev Immunol* 2014; **14**:141–53.
4 Wittkopf N, Neurath MF, Becker C. Immune–epithelial crosstalk at the intestinal surface. *J Gastroenterol* 2014; **49**:375–87.

5 Olszak T, Neves JF, Dowds CM, Baker K, Glickman J, Davidson NO, *et al.* Protective mucosal immunity mediated by epithelial CD1d and IL-10. *Nature* 2014; **509**:497–502.
6 Josefowicz SZ, Lu LF, Rudensky AY. Regulatory T cells: mechanisms of differentiation and function. *Annu Rev Immunol* 2012; **30**:531–64.
7 Burzyn D, Benoist C, Mathis D. Regulatory T cells in nonlymphoid tissues. *Nat Immunol* 2013; **14**:1007–13.
8 Hegazy AN, Powrie F. MICROBIOME. Microbiota RORgulates intestinal suppressor T cells. *Science* 2015; **349**:929–30.
9 Beyersdorf N, Ding X, Tietze JK, Hanke T. Characterization of mouse CD4 T cell subsets defined by expression of KLRG1. *Eur J Immunol* 2007; **37**:3445–54.
10 Feuerer M, Hill JA, Kretschmer K, von Boehmer H, Mathis D, Benoist C. Genomic definition of multiple *ex vivo* regulatory T cell subphenotypes. *Proc Natl Acad Sci USA* 2010; **107**:5919–24.
11 Saito T, Nishikawa H, Wada H, Nagano Y, Sugiyama D, Atarashi K, *et al.* Two $FOXP3^+CD4^+$ T cell subpopulations distinctly control the prognosis of colorectal cancers. *Nat Med* 2016; **22**:679–84.
12 Plitas G, Konopacki C, Wu K, Bos PD, Morrow M, Putintseva EV, *et al.* Regulatory T cells exhibit distinct features in human breast cancer. *Immunity* 2016; **45**:1122–34.
13 De Simone M, Arrigoni A, Rossetti G, Gruarin P, Ranzani V, Politano C, *et al.* Transcriptional landscape of human tissue lymphocytes unveils uniqueness of tumor-infiltrating T regulatory cells. *Immunity* 2016; **45**:1135–47.
14 Libusova L, Stemmler MP, Hierholzer A, Schwarz H, Kemler R. N-cadherin can structurally substitute for E-cadherin during intestinal development but leads to polyp formation. *Development* 2010; **137**:2297–305.
15 Barker N, van Es JH, Kuipers J, Kujala P, van den Born M, Cozijnsen M, *et al.* Identification of stem cells in small intestine and colon by marker gene Lgr5. *Nature* 2007; **449**:1003–7.
16 Harada N, Tamai Y, Ishikawa T, Sauer B, Takaku K, Oshima M, *et al.* Intestinal polyposis in mice with a dominant stable mutation of the β-catenin gene. *EMBO J* 1999; **18**:5931–42.
17 Sanos SL, Diefenbach A. Isolation of NK cells and NK-like cells from the intestinal lamina propria. *Methods Mol Biol* 2010; **612**:505–17.
18 Izcue A, Hue S, Buonocore S, Arancibia-Carcamo CV, Ahern PP, Iwakura Y, *et al.* Interleukin-23 restrains regulatory T cell activity to drive T cell-dependent colitis. *Immunity* 2008; **28**:559–70.
19 Wirtz S, Neufert C, Weigmann B, Neurath MF. Chemically induced mouse models of intestinal inflammation. *Nat Protoc* 2007; **2**:541–6.
20 Maywald RL, Doerner SK, Pastorelli L, De Salvo C, Benton SM, Dawson EP, *et al.* IL-33 activates tumor stroma to promote intestinal polyposis. *Proc Natl Acad Sci USA* 2015; **112**:E2487–96.
21 Lupar E, Brack M, Garnier L, Laffont S, Rauch KS, Schachtrup K, *et al.* Eomesodermin expression in $CD4^+$ T cells restricts peripheral Foxp3 induction. *J Immunol* 2015; **195**:4742–52.
22 Reich M, Liefeld T, Gould J, Lerner J, Tamayo P, Mesirov JP. GenePattern 2.0. *Nat Genet* 2006; **38**:500–1.
23 Gene Ontology Consortium. Gene Ontology Consortium: going forward. *Nucleic Acids Res* 2015; **43**:D1049–56.
24 Cheng G, Yuan X, Tsai MS, Podack ER, Yu A, Malek TR. IL-2 receptor signaling is essential for the development of $Klrg1^+$ terminally differentiated T regulatory cells. *J Immunol* 2012; **189**:1780–91.
25 Tauro S, Nguyen P, Li B, Geiger TL. Diversification and senescence of $Foxp3^+$ regulatory T cells during experimental autoimmune encephalomyelitis. *Eur J Immunol* 2013; **43**:1195–207.
26 Miyara M, Yoshioka Y, Kitoh A, Shima T, Wing K, Niwa A, *et al.* Functional delineation and differentiation dynamics of human $CD4^+$ T cells expressing the FoxP3 transcription factor. *Immunity* 2009; **30**:899–911.
27 Huehn J, Siegmund K, Lehmann JC, Siewert C, Haubold U, Feuerer M, *et al.* Developmental stage, phenotype, and migration distinguish naive- and effector/memory-like $CD4^+$ regulatory T cells. *J Exp Med* 2004; **199**:303–13.
28 Blatner NR, Bonertz A, Beckhove P, Cheon EC, Krantz SB, Strouch M, *et al.* In colorectal cancer mast cells contribute to systemic regulatory T-cell dysfunction. *Proc Natl Acad Sci USA* 2010; **107**:6430–5.
29 Wohlfert EA, Grainger JR, Bouladoux N, Konkel JE, Oldenhove G, Ribeiro CH, *et al.* GATA3 controls $Foxp3^+$ regulatory T cell fate during inflammation in mice. *J Clin Invest* 2011; **121**:4503–15. Epub 2011/10/04.
30 Wang Y, Su MA, Wan YY. An essential role of the transcription factor GATA-3 for the function of regulatory T cells. *Immunity* 2011; **35**:337–48.
31 Rudra D, deRoos P, Chaudhry A, Niec RE, Arvey A, Samstein RM, *et al.* Transcription factor Foxp3 and its protein partners form a complex regulatory network. *Nat Immunol* 2012; **13**:1010–9.
32 Sawant DV, Sehra S, Nguyen ET, Jadhav R, Englert K, Shinnakasu R, *et al.* Bcl6 controls the Th2 inflammatory activity of regulatory T cells by repressing Gata3 function. *J Immunol* 2012; **189**:4759–69.
33 Farin HF, Van Es JH, Clevers H. Redundant sources of Wnt regulate intestinal stem cells and promote formation of Paneth cells. *Gastroenterology* 2012; **143**:1518–29. e7.
34 Clevers H, Nusse R. Wnt/β-catenin signaling and disease. *Cell* 2012; **149**:1192–205.
35 Fridman WH, Pages F, Sautes-Fridman C, Galon J. The immune contexture in human tumours: impact on clinical outcome. *Nat Rev Cancer* 2012; **12**:298–306.
36 Su LK, Kinzler KW, Vogelstein B, Preisinger AC, Moser AR, Luongo C, *et al.* Multiple intestinal neoplasia caused by a mutation in the murine homolog of the APC gene. *Science* 1992; **256**:668–70.
37 Brannon AR, Vakiani E, Sylvester BE, Scott SN, McDermott G, Shah RH, *et al.* Comparative sequencing analysis reveals high genomic concordance between matched primary and metastatic colorectal cancer lesions. *Genome Biol* 2014; **15**:454.
38 Zeineldin M, Neufeld KL. Understanding phenotypic variation in rodent models with germline Apc mutations. *Can Res* 2013; **73**:2389–99.
39 Akeus P, Langenes V, Kristensen J, von Mentzer A, Sparwasser T, Raghavan S, *et al.* Treg-cell depletion promotes chemokine production and accumulation of $CXCR3^+$ conventional T cells in intestinal tumors. *Eur J Immunol* 2015; **45**:1654–66.
40 Schiering C, Krausgruber T, Chomka A, Frohlich A, Adelmann K, Wohlfert EA, *et al.* The alarmin IL-33 promotes regulatory T-cell function in the intestine. *Nature* 2014; **513**:564–8.
41 Nakanishi Y, Seno H, Fukuoka A, Ueo T, Yamaga Y, Maruno T, *et al.* Dclk1 distinguishes between tumor and normal stem cells in the intestine. *Nat Genet* 2013; **45**:98–103.
42 Burzyn D, Kuswanto W, Kolodin D, Shadrach JL, Cerletti M, Jang Y, *et al.* A special population of regulatory T cells potentiates muscle repair. *Cell* 2013; **155**:1282–95.
43 Arpaia N, Green JA, Moltedo B, Arvey A, Hemmers S, Yuan S, *et al.* A distinct function of regulatory T cells in tissue protection. *Cell* 2015; **162**:1078–89.
44 Arteaga CL, Engelman JA. ERBB receptors: from oncogene discovery to basic science to mechanism-based cancer therapeutics. *Cancer Cell* 2014; **25**:282–303.
45 Worthington JJ, Kelly A, Smedley C, Bauche D, Campbell S, Marie JC, *et al.* Integrin $\alpha_v\beta_8$-mediated TGF-β activation by effector regulatory T cells is essential for suppression of T-cell-mediated inflammation. *Immunity* 2015; **42**:903–15.
46 Manetti M, Ibba-Manneschi L, Liakouli V, Guiducci S, Milia AF, Benelli G, *et al.* The IL1-like cytokine IL33 and its receptor ST2 are abnormally expressed in the affected skin and visceral organs of patients with systemic sclerosis. *Ann Rheum Dis* 2010; **69**:598–605.

Supporting Information

Additional Supporting Information may be found in the online version of this article:

Figure S1. (a) Interleukin-2 production by $CD4^+$ $Foxp3^-$ T cells from the spleen or mesenteric lymph nodes (MLN) of $Cdh1^{\Delta IEC}$ mice or control littermates. Data are pooled from two independent experiments. (b) Frequencies of $Foxp3^+$ among $CD4^+$ T cells from mice of the indicated genotypes. (c) Frequencies of $CD103^+$ $KLRG1^-$, $CD103^+$ $KLRG1^+$ and $CD103^-$ $KLRG1^+$ cells, total $CD103^+$ cells and total $KLRG1^+$ cells among colonic $CD4^+$ $Foxp3^+$ T cells from 3-week-old specific pathogen-free (SPF) $Cdh1^{\Delta IEC}$ mice (red) and control littermates (black). Both $CD103^+$ and $CD103^-$ $KLRG1^+$ regulatory T (Treg) cells are increased in $Cdh1^{\Delta IEC}$ mice, whereas $CD103^+$ $KLRG1^-$ Treg cells are not increased. (d) Frequencies of $Foxp3^-$ $KLRG1^+$ among $CD4^+$ T cells (left) and $KLRG1^+$ among $CD3^+$ $CD4^-$ T cells (mostly $CD8^+$ T cells) (right) from 3-week-old SPF $Cdh1^{\Delta IEC}$ mice (red) and $Cdh1^{fl/Ncad}$ control littermates (black). Each point corresponds to an individual mouse. Data are pooled from at least three independent analyses. $*P < 0{\cdot}05$; $**P < 0{\cdot}01$; $***P < 0{\cdot}001$; ns, not significant. (e) Comparison of KLRG1 levels on different $KLRG1^+$ small intestinal lymphoid populations. Solid line: $CD4^+$ $Foxp3^+$ $KLRG1^+$ cells, dotted line: $CD8^+$ $KLRG1^+$ cells,

dashed line: TCRβ^- GATA3^{hi} KLRG1$^+$ ILC2 cells. Grey histogram, control CD4$^+$ Foxp3$^+$ KLRG1$^-$ cells. The frequency of CD4$^+$ Foxp3$^-$ KLRG1$^+$ cells is very low; KLRG1 levels can be seen in Fig. 1(d).

Figure S2. Characteristics of KLRG1$^+$ regulatory T (Treg) cells. (a) KLRG1$^+$ Treg cells are suppressive *in vitro*. CFSE-labelled CD25$^-$ CD4$^+$ T cells were cultured with sorted KLRG1$^-$ or KLRG1$^+$ CD25$^+$ T cells at different ratios. The histograms show CFSE signal after 3 days of culture without Treg cells (grey) or with 1 : 1 KLRG1$^-$ (left plot, black line) or KLRG1$^+$ (central plot, black line) CD25$^+$ T cells. Plots are gated on CFSE$^+$ cells. Right, frequency of divided CFSE$^+$ cells after 3 days of culture with different numbers of KLRG1$^+$ (red) or KLRG1$^-$ (black) CD25$^+$ T cells. Data show mean ± SD of three replicates and they are representative of two independent experiments. (b) Dot plot showing KLRG1 versus IRF4 expression in CD4$^+$ Foxp3$^+$ KLRG1$^+$ Treg cells from colon and small intestine from a Cdh1$^{\Delta IEC}$ mouse; IRF4 showing spleen (non-tissue organ harbouring IRF4$^-$ cells) and colon from a control littermate are shown on top as a reference. (c) Frequencies of Helios-expressing cells among Foxp3$^+$ KLRG1$^-$ (left) and Foxp3$^+$ KLRG1$^+$ (right) cells from control (empty) and littermate specific pathogen-free (SPF) Cdh1$^{\Delta IEC}$ mice (filled symbols). Data shown are pooled from three independent experiments. Each dot represents an individual mouse. (d) Dot plot showing KLRG1 versus Bcl-2 expression in CD4$^+$ Foxp3$^+$ KLRG1$^+$ Treg cells from colon and small intestine from a Cdh1$^{\Delta IEC}$ mouse and control littermate. (e) Frequency of CD44^{hi} CD62L^{lo} among Foxp3$^+$ KLRG1$^-$ (left) and Foxp3$^+$ KLRG1$^+$ (right) from mesenteric lymph nodes of control (black) and littermate SPF Cdh1$^{\Delta IEC}$ mice (red symbols). Data shown are pooled from three independent experiments. Each dot represents an individual mouse. (f) Interleukin-2 (IL-2), interferon-γ, IL-17, IL-5 and IL-13 secretion by CD4$^+$ Foxp3$^+$ KLRG1$^+$ cells from the indicated organs of control (empty) and littermate SPF Cdh1$^{\Delta IEC}$ mice (red symbols). Data shown are pooled from two independent experiments. Each dot represents an individual mouse.

